Multinucleon transfer reactions in the ^{40}Ar+^{208}Pb system

T. Mijatović[1], S. Szilner[1], L. Corradi[2], D. Montanari[3,4], G. Pollarolo[5], E. Fioretto[2],
A. Gadea[6], A. Goasduff[2], D. Jelavić Malenica[1], N. Mărginean[7], M. Milin[8], G. Montagnoli[3],
F. Scarlassara[3], N. Soić[1], A. M. Stefanini[2], C. A. Ur[7], and J. J. Valiente-Dobón[2]

[1]*Ruđer Bošković Institute, Zagreb, Croatia*
[2]*Istituto Nazionale di Fisica Nucleare, Laboratori Nazionali di Legnaro, Legnaro, Italy*
[3]*Dipartimento di Fisica, Università di Padova, and Istituto Nazionale di Fisica Nucleare, Padova, Italy*
[4]*Institut Pluridisciplinaire Hubert Curien, CNRS-IN2P3, Université de Strasbourg, Strasbourg, France*
[5]*Dipartimento di Fisica Teorica, Università di Torino,*
and Istituto Nazionale di Fisica Nucleare, Torino, Italy
[6]*Instituto de Fisica Corpuscular, CSIC-Universitat de València, Valencia, Spain*
[7]*Horia Hulubei National Institute of Physics and Nuclear Engineering, Bucharest, Romania and*
[8]*Department of Physics, Faculty of Science, University of Zagreb, Zagreb, Croatia*
(Dated: December 3, 2016)

We measured multinucleon transfer reactions in the ^{40}Ar+^{208}Pb system at an energy close to the Coulomb barrier, by employing the PRISMA magnetic spectrometer. We extracted differential and total cross sections of the different transfer channels, with a careful investigation of the total kinetic energy loss distributions. A comparison between different systems having the same ^{208}Pb target and with projectiles going from neutron-poor to neutron-rich nuclei, i.e., ^{40}Ca, ^{58}Ni, and ^{40}Ar, as well as between the data and GRAZING calculations have been carried out. The neutron-rich (stable) ^{40}Ar beam allowed us to get access to the channels involving proton pick-up, whose behaviour in connection with the production of neutron-rich heavy partner has been outlined.

I. INTRODUCTION

Transfer reactions have always been of great importance for nuclear structure and nuclear reaction mechanism studies [1–4]. With heavy ions it becomes feasible, in a single collision, to transfer several nucleons and a considerable amount of energy and angular momenta from the relative motion to the intrinsic degrees of freedom [1]. In this way it is possible to follow how the mechanism evolves from the quasi-elastic to the more complex deep-inelastic and to fusion. In the quasi-elastic regime the mass and charge distributions of transfer products are governed by optimum Q-value considerations and transfer form factors. For nuclei close to the stability line, these optimum Q-value arguments favor the neutron pick-up and the proton stripping channels (pick-up and stripping are referring to the lighter reaction fragment) [5–9]. This is the reason why multinucleon transfer reactions have recently been used as a competitive tool for the production of neutron-rich nuclei in the vicinity of the light partner (see for example Refs. [10–13]).

When using neutron-rich projectiles also proton pick-up and neutron stripping channels open up, giving the possibility to populate neutron-rich heavy partners [5]. It is important to probe these predictions by studying systems which are apt to populate also the proton pick-up sector. Few studies have been performed so far where proton pick-up channels have been measured at energies close to the Coulomb barrier and completely identified in Z, A and Q-value. Measurements have been performed in the ^{144}Sm+^{88}Sr [14] and ^{48}Ca+^{124}Sn [15] cases, where main focus was on studies of nucleon correlation effects.

Data sets have been extracted using ^{238}U targets in the ^{64}Ni+^{238}U [16] and ^{136}Xe+^{238}U [17] systems, where, in particular, studies of the influence of secondary processes on multinucleon transfer were carried out. We point out that, in general for heavy systems, the presence of fission, especially from ^{238}U, may contaminate genuine transfer channels and has to be taken into account. Very recently a high resolution measurement has been performed in the ^{136}Xe+^{198}Pt system [18] to study the population yields of neutron-rich nuclei.

In the present work we show a comprehensive study of the multinucleon transfer reaction ^{40}Ar+^{208}Pb measured near the Coulomb barrier. By using the most neutron-rich stable ^{40}Ar we could populate, besides neutron pick-up and proton stripping channels, also neutron stripping and proton pick-up channels. We used the double magic ^{208}Pb target since it is weakly affected by the presence of other mechanisms, i.e., fission. We provide differential and total cross sections and total kinetic energy loss distributions, measured with the large solid angle magnetic spectrometer PRISMA [19, 20]. This was achieved by consistently matching for the first time three angular and magnetic field settings. To deal with the wealth of produced transfer channels in a large kinetic energy range we took into account the spectrometer's response function. Data have been compared with calculations performed with the GRAZING code [21–23], which was already successfully used in the study of different systems.

The paper is entirely devoted to the study of the multinucleon transfer reaction mechanism. The same reaction (in the same experiment) was previously used [12, 24]

to study the spectroscopy of the neutron-rich Ar and Cl isotopes with PRISMA coupled with the CLARA gamma array.
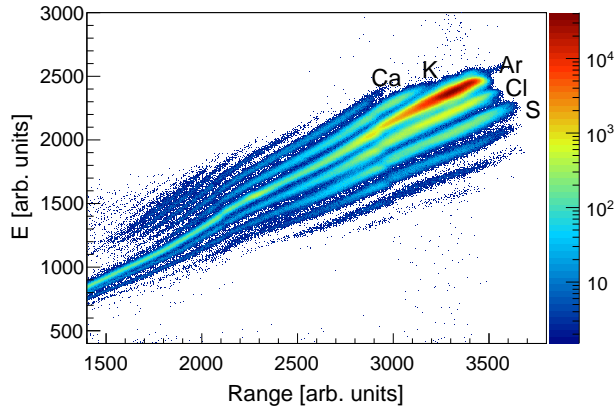
II. EXPERIMENTAL RESULTS

FIG. 1: (Color online) Matrix of Range versus energy E for the ^{40}Ar+^{208}Pb reaction at $E_{\text{lab}} = 6.4$ MeV/A and at $\theta_{\text{lab}} = 54°$. The Range has been determined using the angle and position information of the ions entering the ionization chamber, together with the different IC sub-anodes information. The most intense band corresponds to Ar ions, with proton pick-up and proton stripping channels visible above and below Ar.

An ^{40}Ar beam was accelerated at $E_{\text{lab}} = 6.4$ MeV/A with an average current of $\sim$ 7 pnA onto a 300 μg/cm^2 strip ($\sim$ 2 mm) ^{208}Pb target, employing the positive ion injector PIAVE coupled to the ALPI post accelerator of LNL. Target isotopic purity was 99.9%. We detected Ar-like fragments in PRISMA at the three angular settings $\theta_{\text{lab}} = 46°$, $54°$ (grazing angle) and $59°$, which, taking into account the large spectrometer acceptance, allowed to construct differential cross sections for the transfer channels in a wide angular range. We here briefly list the main characteristics of the spectrometer [19, 20] and its detector system. A position-sensitive micro-channel plate detector [25] is placed at the entrance of the spectrometer, providing a start signal for time-of-flight measurements and bi-dimensional position signals. Ions pass through the optical elements of the spectrometer (a quadrupole and a dipole) and enter a focal plane detector [26] which is made of a parallel plate detector of multi-wire type, providing timing and bi-dimensional position signals with resolutions similar to the entrance detector. Located at the end of the focal plane is an array of a transverse field multi-parametric ionization chambers (IC), providing nuclear charge via energy loss (ΔE) and total energy (E) measurements. The detector system gives all the necessary information for the complete ion identification, which is performed via an event-by-event

reconstruction of the trajectory inside the magnetic elements [27]. In order to obtain the optimum nuclear charge (Z) resolution, the direction followed by the different ions reaching the IC in a broad range of kinetic energies and directions was taken into account. The result is illustrated in Fig. 1, which shows the range versus energy matrix. Separation between ions of different Z is clearly visible, with the most intense band corresponding to Ar ions, and with proton pick-up and stripping channels appearing above and below Ar, respectively.
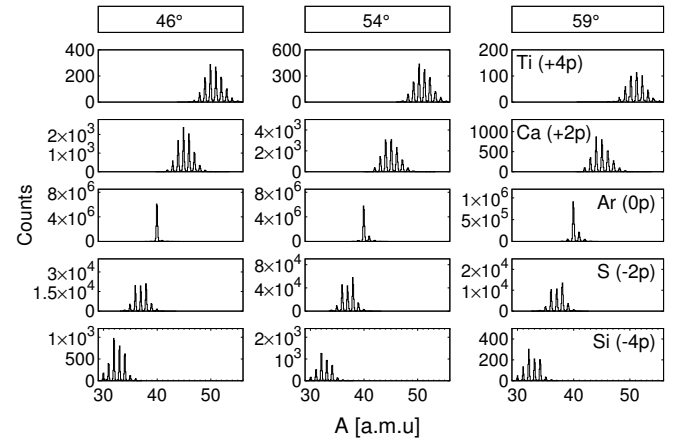

FIG. 2: Mass spectra for the transfer products measured in the ^{40}Ar+^{208}Pb reaction, spanning the range from $(+4p)$ to $(-4p)$ channels for even Z isotopes for the three measured angles.

Mass spectra for the different identified isotopes are presented in Fig. 2, separately for all the three measured angles. Being ^{40}Ar the most neutron-rich stable isotope, we could populate pick-up and stripping of both neutrons and protons, as clearly visible from the quite symmetric distribution around ^{40}Ar. One observes that close to the entrance channel mass partition the relative strength of the different channels is compatible with the quasi-elastic character of the reaction, mainly governed by optimum Q values and nuclear structure properties (form factors). For the channels involving pick-up of protons, the reaction favours the neutron pick-up region. Moreover, for the channels far from the entrance channel mass partition the distributions become wider and Gaussian-like shaped, reflecting also the presence of large energy loss components, convoluted with the energy acceptance of the spectrometer. These large energy losses may lead to neutron evaporation which strongly affects the lower mass region of all populated isotopes.

To be able to describe the charge and mass distributions in a peripheral collision between two heavy ions, like the one shown above, one has to appeal to contributions from three different reaction mechanisms, direct transfer, deep-inelastic (where mass and charge are exchanged in a diffusion-like mechanism) and neutron evaporation (for each charge this mechanism regulates the distributions of the lighter masses). Some insight into the role
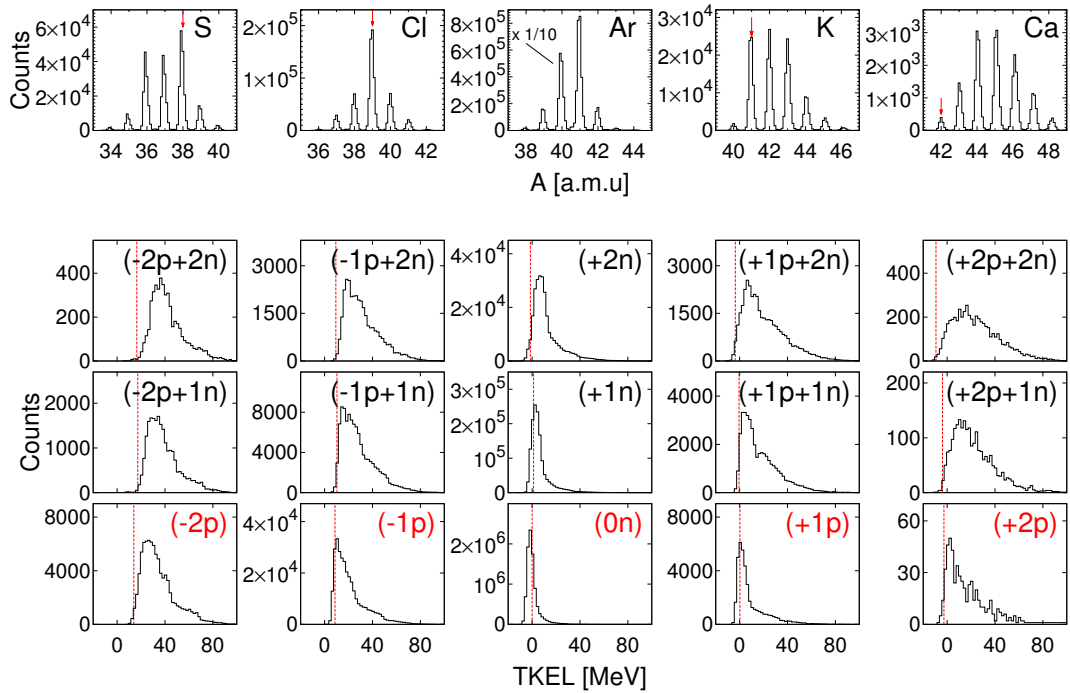
FIG. 3: (Color online) Experimental TKEL spectra for the indicated transfer channels at $\theta_{\mathrm{lab}} = 54°$. The vertical dashed lines represent the ground state Q values. In the top row the mass spectra for each Z are also depicted, with the red arrows indicating the pure proton transfer channels. The ^{40}Ar peak has been scaled down by a factor 10 to better display the behaviour of the transfer channels.

of these mechanisms can be gained by studying in detail the Total Kinetic Energy Loss (TKEL) and angular distributions that provide information on the "hardness" of the collision and on its contact time.

The TKEL were constructed assuming a pure binary process and imposing the conservation of momentum. The excitation energies of both reaction partners are embedded into these TKEL. The experimental TKEL distributions are shown in Fig. 3 for PRISMA positioned at 54°, where in the top row are also depicted the mass spectra for each Z. One can clearly follow the evolution pattern as a function of the number of transferred neutrons and protons. The few nucleon transfer channels display narrow peaks close to the optimum Q-value, typical of the quasi-elastic regime. The pure neutron transfer channels, in particular, have major contribution close to the optimum Q-value (~ 0 MeV) with an increasing strength for large energy losses as more neutrons are transferred. The trend is quite similar also for pure proton transfers where larger energy losses are reached when more protons are transferred. For channels that involve also the exchange of neutrons, especially in the proton pick-up region, the TKEL distributions look all quite similar, with a centroid at large energy losses.

The large acceptance of PRISMA allows us to study the wealth of the transfer channels and their associated TKEL with a single setting of magnetic fields. Of course, for the cases where very large energy losses are involved,
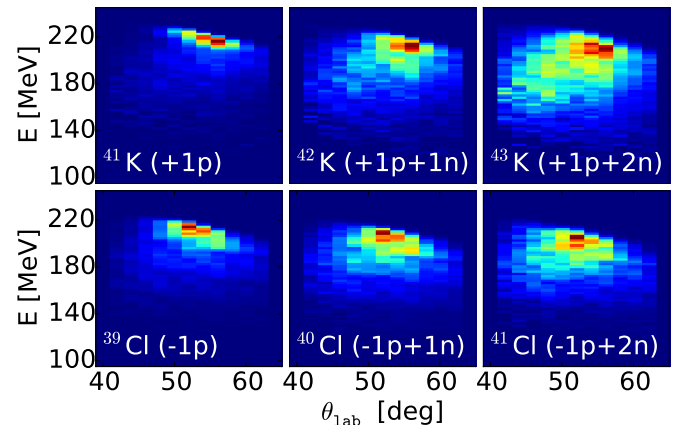

FIG. 4: (Color online) Wilczynski plots, kinetic energy E in the laboratory system versus θ_{lab}, for selected channels in the ^{40}Ar+^{208}Pb reaction. The plots have been obtained by matching the measured events at the three PRISMA angular and magnetic settings.

the shape of the TKEL spectra may be modified to some extent by the acceptance of the spectrometer, yet allowing for a qualitative interpretation of the evolution of the reaction from the quasi-elastic to the deep-inelastic regimes. This evolution can be followed in the Wilczynski plots (kinetic energy E in the laboratory system versus

θ_{lab}), shown in Fig. 4 for selected channels with sufficient statistics. They have been obtained by matching the three angular and magnetic settings of the spectrometer, and corrected for the PRISMA response [28, 29]. This was achieved by using a Monte Carlo simulation of the ion trajectories, incorporating the kinematics of the reaction and the geometry of the magnetic elements and detectors [28, 29]. For one particle transfer channels the main strength concentrates in a narrow band ($\sim$ 10 MeV wide) close to the largest kinetic energy (i.e., smallest TKEL). For the transfers of more particles, one sees a widening of these bands and the appearance of the large TKEL, especially at more forward angles. The contribution of the large TKEL components is more pronounced for the proton pick-up channels, and when more nucleons are transferred. This is especially evident for the ($+1p + 2n$) channel where the large TKEL components already present a significant fraction of the distribution. Such behaviour may indicate that processes more complex than the direct transfer dominate the observed yields.

The experimental angular distributions integrated over the full TKEL range are shown in Fig. 5 together with the GRAZING calculations (see below). These angular distributions were measured in the wide angular range $\Delta\theta_{\text{lab}} = 41° - 62°$, thus covering most of the total transfer strength. As previously explained, they have also been obtained by matching the three angular and magnetic settings of the spectrometer. Corrections for the PRISMA response have been applied to each experimental differential cross section, following the procedure outlined in Ref. [29] to which we refer for the details. This procedure turned out to be essential at the borders of the spectrometer. The absolute scale of cross sections was obtained by normalizing the quasi-elastic ^{40}Ar events to the Rutherford cross section at forward angles [28, 29].

From Fig. 5 one sees that for one- and two-nucleon transfer the angular distributions are bell shaped, centered at the grazing angle, and weakly isotope dependent, as expected in the quasi-elastic regime. When more nucleons are transferred, and especially for the proton pick-up channels, the distributions broaden and increase at forward angles indicating the contribution from deep-inelastic collision (large energy losses), i.e., from collisions deriving from smaller impact parameters. These components at large energy loss may be affected by the energy acceptance of the spectrometer, and thus not fully corrected for the PRISMA response. Figure 5 also displays the transfer channels involving the "stripping" of neutrons (bottom row). Here one notices that the angular distributions are all centered at the same angle as the pure proton channels. Such behaviour indicates the dominance of neutron evaporation in their population mechanism. In general it is difficult to disentangle the quasi-elastic and deep-inelastic components, since they may strongly overlap. At least in some cases these components could be separated, as for instance for the ($-1p + 1n$), ($+1p + 1n$) and ($+1p + 2n$) channels, visible in the Wilczynski plot of Fig. 4 and in the projected spectra (Fig. 3). In order to better understand the behaviour of the angular distributions, from these kind of channels we extracted the quasi-elastic components by taking into account the ground-to-ground state Q values and by integrating the energy excitation regions up to $\sim$ 20 MeV. The reliability of the method has been tested by employing different separation procedures to integrate the two distributions. This procedure has been followed for each scattering angle.

This is illustrated in Fig. 6 where we plot the distributions for two representative channels, the ($+1n$) and ($+1p+2n$) ones. The distributions have been obtained by integrating over the whole TKEL (black empty points) and only over the quasi-elastic part (red full points). In the case of the pure one-neutron transfer channel the two distributions are very similar, being most of the strength of quasi-elastic character. At variance with the ($+1n$) channel, a typical rather broad and forward rising distribution is observed for the ($+1p + 2n$) channel when integrating over the full TKEL range. On the other hand, its quasi-elastic distribution (red full points) turns out to be more similar in shape to the one for the ($+1n$) channel. This quasi-elastic energy range is also where, in general, the three different PRISMA settings match more smoothly, being the range less influenced by the spectrometer's acceptance.

III. COMPARISON WITH GRAZING PREDICTIONS

Figure 7 (top raw) shows the experimental total cross sections for the indicated channels obtained by integrating the angular distributions via Gaussian fits, over the full TKEL range. In the same Fig. 7 we also report, for comparison, the total cross sections for other previously measured multinucleon transfer channels having ^{208}Pb as target. The reaction with ^{208}Pb is in fact a suitable case that is weakly affected by the presence of other mechanisms (i.e., fission) and, ^{208}Pb being a doubly magic nucleus, calculations can be performed in a more reliable way. We include two cases, one with the closed shell ^{40}Ca [7] and one with the open shell ^{58}Ni projectile [6]. These multinucleon transfer reactions were measured with the time-of-flight spectrometer PISOLO [16, 30] at LNL. The ^{40}Ca+^{208}Pb data are from the highest measured energy reported in Ref. [7]. In the case of the ^{58}Ni+^{208}Pb [6] system the data are published for $E_{\text{lab}} = 328.4$ MeV, but we took the opportunity to re-analyze the data measured at the highest (unpublished) energy $E_{\text{lab}} = 346$ MeV which is more pertinent for an overall comparison of all three systems at similar energies above the Coulomb barrier. We point out that in those measurements we observed traces of proton pick-up channels (see e.g. the corresponding Z-A two-dimensional plots of Refs. [6, 7]). We were able to estimate that the mass integrated yields for the ($+1p$) channels are of the same order as for ($-6p$).
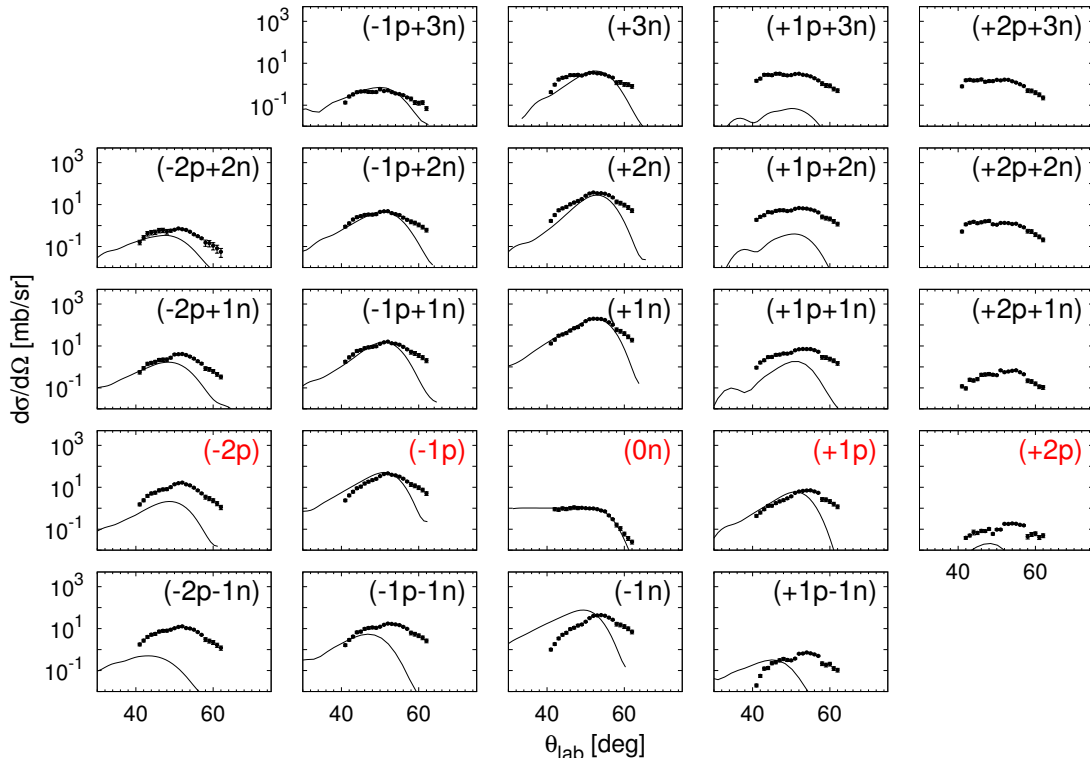
FIG. 5: Experimental (points) and GRAZING calculated (curves) angular distributions for the indicated transfer channels. The experimental distributions have been integrated over the full TKEL. The $(0n)$ channel corresponds to the elastic(+inelastic) channel, plotted as a ratio to the Rutherford cross section.
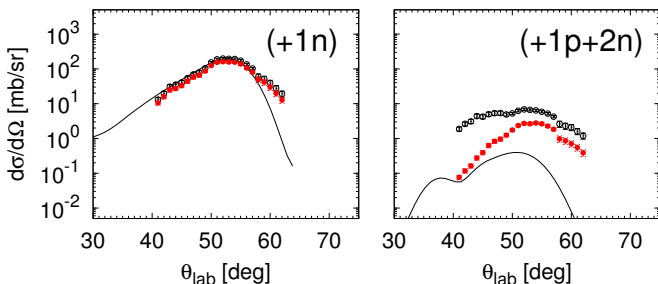

FIG. 6: (Color online) Experimental angular distributions of the $(+1n)$ and $(+1p + 2n)$ channels integrated over the full TKEL range (black empty points) and integrated over the quasi-elastic part with the TKEL ≤ 20 MeV (red full points). The results of the GRAZING calculations are also plotted (curves).

This comparison between different systems, and between the data and calculations, is significant for understanding the importance of the different degrees of freedom that influence the evolution of the reaction.

The data have been compared with calculations performed with the GRAZING [21–23] model. This model calculates the evolution of the reaction by taking into account, besides the relative motion variables, the intrinsic degrees of freedom of projectile and target. These are the surface degrees of freedom and the one-nucleon transfer channels. The relative motion of the system is calculated in a nuclear plus Coulomb field. The exchange of many nucleons proceeds via a multi-step mechanism of single nucleons (both, protons and neutrons, via stripping, and pick-up processes). This model has been so far successfully applied in the description of multinucleon transfer reactions [6–8] as well as of fusion reactions and barrier distributions [31].

In the ^{40}Ar$+^{208}$Pb system GRAZING particularly well describes the one nucleon transfer channels, $(\pm 1n)$ and $(\pm 1p)$, as also visible in the differential cross sections of Fig. 5. In fact the TKEL distributions of these channels are mainly concentrated in a narrow peak in the low energy region. Other pure neutron transfer channels also show well reproduced differential and total cross sections. This is particularly true for neutron pick-up channels. For the neutron stripping channels one notices a shift of angular distribution centroids and some overestimation of the total cross sections. As discussed previously, when neutron "stripping" are involved, we have to keep in mind that the evaporation of neutrons plays a very important role. Deviations between experimental data and calculations are more marked for channels involving the transfer of many protons. This fact has been discussed in previous publications [6, 7] where experimental cross sections were
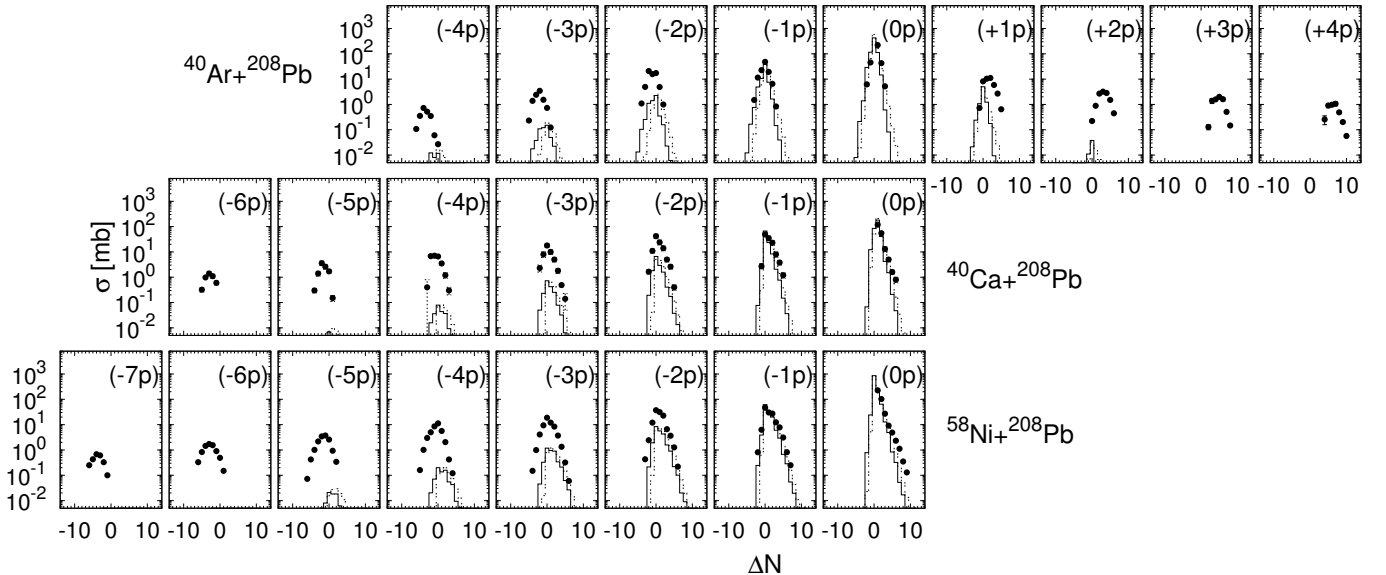
FIG. 7: Total experimental cross section for ^{40}Ar, ^{40}Ca, and ^{58}Ni induced reactions on the ^{208}Pb target, at beam energies $E_{\text{lab}} = 6.4$, 6.2, and 6 MeV/A, respectively, (points) and the GRAZING calculations with (full line) and without (dashed line) neutron evaporation.

compared with different semi-classical models in order to see if the addition of new modes, in particular the transfer of a pair of nucleon (both neutrons and protons), may be justified. The inclusion of these pair-transfer modes may be essential. However, we cannot rule out the contribution from deep-inelastic processes as we move away from the entrance channel mass partition, as can be followed in the flattening of the angular distributions and widening of the TKEL.

The deviations between experimental data and calculations are more pronounced in the proton pick-up sector, in particular when neutron pick-up channels are involved. As it is seen from the corresponding TKEL spectra, they are very broad and centered at much larger energy losses, so that the contributions from the deep-inelastic collision are very substantial. We stress that the proton transfer processes in a heavy-ion collisions are much less understood than the ones of neutrons, since large modification in the trajectories of entrance and exit channels are involved (due to the modification of the Coulomb field). The single particle level density for protons is less studied than the one of neutrons and the corresponding single-particle form factors are less known (even the one-proton transfer cross sections are not very well described in the DWBA, in fact this theory predicts angular distributions that are shifted in comparison with the data). Certainly, the theory has to improve the description of proton transfer channels. Thus, any quantitative conclusion derived from the comparison shown in Figs. 5 and 7 for the proton pick-up channels has to be taken with great care at this stage.

A similar situation in the proton pick-up sector has been observed in the recently measured ^{136}Xe+^{198}Pt sys-

tem in GANIL [18] using the most neutron-rich stable ^{136}Xe isotope. In this system, using heavier projectiles, a wider Z-N distribution is observed with strong proton pick-up channels. It has been shown how this transfer path leads to the population of neutron-rich Hg and Os nuclei when a low TKEL cut is applied. Thus, this path, i.e., proton pick-up and neutron stripping, is particularly relevant for the population of neutron-rich heavy partner.

The measured Z-N distributions for the three discussed ^{58}Ni,^{40}Ca,^{40}Ar+^{208}Pb systems can be better appreciated from the bi-dimensional plots of Fig. 8. While with the neutron poor ^{40}Ca and ^{58}Ni beams the reaction mechanism strongly favors the proton stripping and neutron pick-up channels, it is evident how the transfer flux changes with the use of the neutron-rich (stable) ^{40}Ar beam. In particular one sees how proton pick-up channels open up. Even if these proton pick-up channels have lower cross sections than the proton stripping ones, the observed Z-N distribution turns out to be more symmetric. A definite dominance of the proton pick-up and neutron stripping channels [5] in the distribution of the transfer flux is predicted to occur with an additional increase of the neutron excess in projectile. Such a situation leads to the population of neutron-rich nuclei in the corresponding heavy partner. One has to keep in mind that the primary yield can be influenced by secondary processes that generally shift the mass distributions toward lower values.

With the presently studied system we provided an experimental evidence on how the transfer flux changes its trend when going from neutron-poor to neutron-rich projectiles on a heavy target. Such a behaviour indicates the importance of multinucleon transfer processes for the
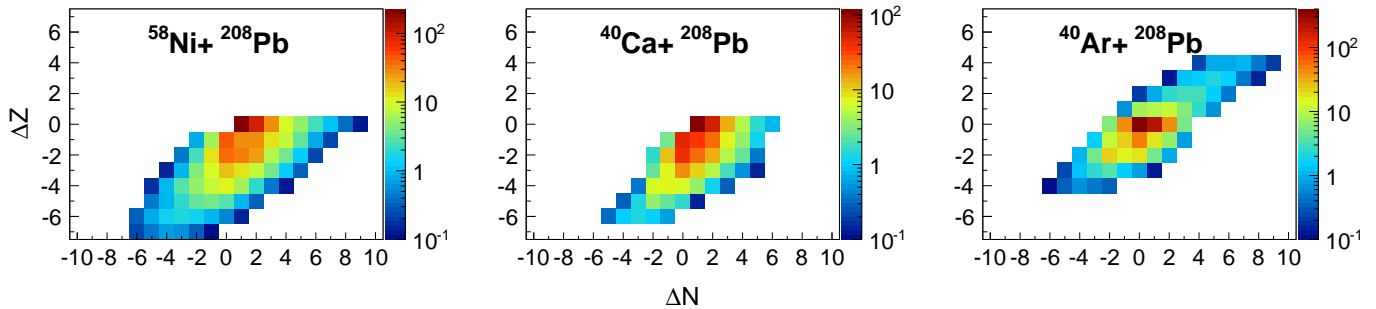
FIG. 8: (Color online) Angle and energy integrated total cross section for ^{40}Ar, ^{40}Ca, and ^{58}Ni projectiles on the ^{208}Pb target, at energies $E_{\text{lab}} = 6.4$, 6.2, and 6 MeV/A, respectively. The cross section values of the elastic(+inelastic) channel, with ΔN and $\Delta Z = 0$, have been scaled down by a factor 100 to better display the behaviour of the transfer channels.

population of moderately neutron-rich isotopes in vicinity of the lighter partner as well as for the population of neutron-rich target-like isotopes with the use of neutron-rich beams.

IV. SUMMARY

The ^{40}Ar+^{208}Pb multinucleon transfer reaction was measured at an energy above the barrier by employing the PRISMA magnetic spectrometer. For channels involving both proton stripping and pick-up, differential and total cross sections and total kinetic energy loss distributions have been obtained by matching three angular and magnetic settings. The experimental observables have been compared with the GRAZING model for transfer reactions, showing the present understanding of these complicated processes. Much more work is needed to properly understand, both theoretically and experimentally, the behavior of proton transfer channels, in particular the proton pick-up ones. The comparison of systems going from the neutron-poor ^{40}Ca and ^{58}Ni to the neutron-rich ^{40}Ar projectiles on ^{208}Pb target shows how

the population trend evolves from proton stripping and neutron pick-up to the opposite direction. Such processes are relevant for the production of neutron-rich target-like nuclei. Investigations on this subject, for reaction mechanism as well as nuclear spectroscopy, are of particular relevance in ongoing and future studies with radioactive beams.

[1] A. Bohr and B. Mottelson, *Nuclear Structure*, edited by W. A. Benjamin (Inc., New York, 1969).
[2] R. A. Broglia, O. Hansen, and C. Riedel, *Advances in Nuclear Physics*, edited by M. Baranger and E. Vogt, (Plenum, New York, 1973), Vol. 6, p. 287.
[3] R. A. Broglia and A. Winther, *Heavy Ion Reactions* (Addison-Wesley Pub. Co., Redwood City CA, 1991).
[4] M. Igarashi, K. Kubo, and K. Tagi, Phys. Rep. **199**, 1 (1991).
[5] C. H. Dasso, G. Pollarolo, and A. Winther, Phys. Rev. Lett. **73**, 1907 (1994).
[6] L. Corradi, A. M. Vinodkumar, A. M. Stefanini, E. Fioretto, G. Prete, S. Beghini, G. Montagnoli, F. Scarlassara, G. Pollarolo, F. Cerutti, and Aage Winther, Phys. Rev. C **66**, 024606 (2002).
[7] S. Szilner, L. Corradi, G. Pollarolo, S. Beghini, B.R. Be-

hera, E. Fioretto, A. Gadea, F. Haas, A. Latina, G. Montagnoli, F. Scarlassara, A. M. Stefanini, M. Trotta, A. M. Vinodkumar, and Y. Wu, Phys. Rev. C **71**, 044610 (2005).
[8] L. Corradi, G. Pollarolo, and S. Szilner, J. of Phys. G: Nucl. Part. Phys. **36**, 113101 (2009).
[9] D. Montanari, L. Corradi, S. Szilner, G. Pollarolo, E. Fioretto, G. Montagnoli, F. Scarlassara, A. M. Stefanini, S. Courtin, A. Goasduff, F. Haas, D. Jelavić Malenica, C. Michelagnoli, T. Mijatović, N. Soić, C. A. Ur, and M. Varga Pajtler, Phys. Rev. Lett. **113**, 052501 (2014).
[10] S. Lunardi, S. M. Lenzi, F. Della Vedova, E. Farnea, A. Gadea, N. Mărginean, D. Bazzacco, S. Beghini, P. G. Bizzeti, A. M. Bizzeti-Sona, D. Bucurescu, L. Corradi, A. N. Deacon, G. de Angelis, E. Fioretto, S. J. Freeman, M. Ionescu-Bujor, A. Iordachescu, P. Mason, D. Mengoni,

G. Montagnoli, D. R. Napoli, F. Nowacki, R. Orlandi, G. Pollarolo, F. Recchia, F. Scarlassara, J. F. Smith, A. M. Stefanini, S. Szilner, C. A. Ur, J. J. Valiente-Dobón, and B. J. Varley, Phys. Rev. C **76**, 034303 (2007).

[11] J. J. Valiente-Dobón, D. Mengoni, A. Gadea, E. Farnea, S. M. Lenzi, S. Lunardi, A. Dewald, Th. Pissulla, S. Szilner, R. Broda, F. Recchia, A. Algora, L. Angus, D. Bazzacco, G. Benzoni, P. G. Bizzeti, A. M. Bizzeti-Sona, P. Boutachkov, L. Corradi, F. Crespi, G. de Angelis, E. Fioretto, A. Grgen, M. Gorska, A. Gottardo, E. Grodner, B. Guiot, A. Howard, W. Królas, S. Leoni, P. Mason, R. Menegazzo, D. Montanari, G. Montagnoli, D. R. Napoli, A. Obertelli, T. Pawlat, G. Pollarolo, B. Rubio, E. Sahin, F. Scarlassara, R. Silvestri, A. M. Stefanini, J. F. Smith, D. Steppenbeck, C. A. Ur, P. T. Wady, J. Wrzesiński, E. Maglione, and I. Hamamoto, Phys. Rev. Lett. **102**, 242502 (2009).

[12] S. Szilner, L. Corradi, F. Haas, D. Lebhertz, G. Pollarolo, C. A. Ur, L. Angus, S. Beghini, M. Bouhelal, R. Chapman, E. Caurier, S. Courtin, E. Farnea, E. Fioretto, A. Gadea, A. Goasduff, D. Jelavić Malenica, V. Kumar, S. Lunardi, N. Mărginean, P. Mason, D. Mengoni, G. Montagnoli, F. Nowacki, F. Recchia, E. Sahin, M.-D. Salsac, F. Scarlassara, R. Silvestri, J. F. Smith, N. Soić, A. M. Stefanini, and J. J. Valiente-Dobón, Phys. Rev. C **84**, 014325 (2011).

[13] R. Chapman, Z. M. Wang, M. Bouhelal, F. Haas, X. Liang, F. Azaiez, B. R. Behera, M. Burns, E. Caurier, L. Corradi, D. Curien, A. N. Deacon, Zs. Dombradi, E. Farnea, E. Fioretto, A. Gadea, A. Hodsdon, F. Ibrahim, A. Jungclaus, K. Keyes, V. Kumar, S. Lunardi, N. Marginean, G. Montagnoli, D. R. Napoli, F. Nowacki, J. Ollier, D. O'Donnell, A. Papenberg, G. Pollarolo, M.-D. Salsac, F. Scarlassara, G. Simpson, J. F. Smith, K. M. Spohr, M. Stanoiu, A. M. Stefanini, S. Szilner, M. Trotta, and D. Verney, Phys. Rev. C **93**, 044318 (2016).

[14] R. Künkel, W. von Oertzen, H. G. Bohlen, B. Gebauer, H. A. Bösser, B. Kohlmeyer, J. Speer, F. Pühlhofer, and D. Schüll, Z. Phys. A **336**, 71 (1990).

[15] L. Corradi, A. M. Stefanini, J. H. He, S. Beghini, G. Montagnoli, F. Scarlassara, G. F. Segato, G. Pollarolo, C.H. Dasso, Phys. Rev. C **56**, 938 (1997).

[16] L. Corradi, A. M. Stefanini, C. J. Lin, S. Beghini, G. Montagnoli, F. Scarlassara, G. Pollarolo, and A. Winther, Phys. Rev. C **59**, 261 (1999).

[17] A. Vogt, B. Birkenbach, P. Reiter, L. Corradi, T. Mijatović, D. Montanari, S. Szilner, D. Bazzacco, M. Bowry, A. Bracco, B. Bruyneel, F. C. L. Crespi, G. de Angelis, P. Désesquelles, J. Eberth, E. Farnea, E. Fioretto, A. Gadea, K. Geibel, A. Gengelbach, A. Giaz, A. Gorgen, A. Gottardo, J. Grebosz, . Hess, P. R. John, J. Jolie, D. S. Judson, A. Jungclaus, W. Korten, S. Leoni, S. Lunardi, R. Menegazzo, D. Mengoni, C. Michelagnoli, G. Montagnoli, D. Napoli, L. Pellegri, G. Pollarolo, A. Pullia, B. Quintana, F. Radeck, F. Recchia, D. Rosso, E. Sahin, M. D. Salsac, F. Scarlassara, P.-A. Soderstrom, A. M. Stefanini, T. Steinbach, O. Stezowski, B. Szpak, Ch. Theisen, C. Ur, J. J. Valiente-Dobón, V. Vandone, and A. Wiens, Phys. Rev. C **92**, 024619 (2015).

[18] Y. X. Watanabe, Y. H. Kim, S. C. Jeong, Y. Hirayama, N. Imai, H. Ishiyama, H. S. Jung, H. Miyatake, S. Choi, J. S. Song, E. Clement, G. de France, A. Navin, M. Rejmund, C. Schmitt, G. Pollarolo, L. Corradi, E. Fioretto, D. Montanari, M. Niikura, D. Suzuki, H. Nishibata, and J. Takatsu, Phys. Rev. Lett. **115**, 172503 (2015).

[19] A. M. Stefanini, L. Corradi, G. Maron, A. Pisent, M. Trotta, A. M. Vinodkumar, S. Beghini, G. Montagnoli, F. Scarlassara, G. F. Segato, A. De Rosa, G. Inglima, D. Pierroutsakou, M. Romoli, M. Sandoli, G. Pollarolo, and A. Latina, Nucl. Phys. **A701**, 217c (2002).

[20] L. Corradi, S. Szilner, G. Pollarolo, D. Montanari, E. Fioretto, A. Stefanini, J. Valiente-Dobón, E. Farnea, C. Michelagnoli, G. Montagnoli, F. Scarlassara, C. Ur, T. Mijatović, D. J. Malenica, N. Soić, and F. Haas, Nucl. Instr. and Meth. in Phys. Res. B **317**, 743 (2013).

[21] A. Winther, Nucl. Phys. A **572**, 191 (1994).

[22] A. Winther, Nucl. Phys. A **594**, 203 (1995).

[23] Program GRAZING, http:/www.to.infn.it/~nanni/grazing.

[24] S. Szilner, L. Corradi, F. Haas, G. Pollarolo, L. Angus, S. Beghini, M. Bouhelal, R. Chapman, E. Caurier, S. Courtin, E. Farnea, E. Fioretto, A. Gadea, A. Goasduff, D. Jelavić Malenica, V. Kumar, S. Lunardi, N. Mărginean, D. Mengoni, T. Mijatović, G. Montagnoli, F. Recchia, E. Sahin, M.-D. Salsac, F. Scarlassara, J. F. Smith, N. Soić, A. M. Stefanini, C. A. Ur, and J. J. Valiente-Dobón, Phys. Rev. C **87**, 054322 (2013).

[25] G. Montagnoli, A.M. Stefanini, M. Trotta, S. Beghini, M. Bettini, F. Scarlassara, V. Schiavon, L. Corradi, B. R. Behera, R. Fioretto, A. Gadea, A. Latina, S. Szilner, L. Donà, M. Rigato, N. A. Kondratiev, A. Yu. Chizhov, G. Kniajeva, E. M. Kozulin, I. V. Pokrovskiy, V. M. Voshressensky, and D. Ackermann, Nucl. Instr. and Meth. in Phys. Res. A **547**, 455 (2005).

[26] S. Beghini, L. Corradi, E. Fioretto, A. Gadea, A. Latina, G. Montagnoli, F. Scarlassara, A. M. Stefanini, S. Szilner, M. Trotta, and A. M. Vinodkumar, Nucl. Instr. and Meth. in Phys. Res. A **551**, 364 (2005).

[27] S. Szilner, C. A. Ur, L. Corradi, N. Marginean, G. Pollarolo, A. M. Stefanini, S. Beghini, B. R. Behera, E. Fioretto, A. Gadea, B. Guiot, A. Latina, P. Mason, G. Montagnoli, F. Scarlassara, M. Trotta, G. de Angelis, F. Della Vedova, E. Farnea, F. Haas, S. Lenzi, S. Lunardi, R. Marginean, R. Menegazzo, D. R. Napoli, M. Nespolo, I. V. Pokrovsky, F. Recchia, M. Romoli, M.-D. Salsac, N. Soić, and J. J. Valiente-Dobón, Phys. Rev. C **76**, 024604 (2007).

[28] D. Montanari, E. Farnea, S. Leoni, G. Pollarolo, L. Corradi, G. Benzoni, E. Fioretto, A. Latina, G. Montagnoli, F. Scarlassara, R. Silvestri, A. M. Stefanini, and S. Szilner, Eur. Phys. J. A **47**, 4 (2011).

[29] T. Mijatović, S. Szilner, L. Corradi, D. Montanari, G. Pollarolo, E. Fioretto, A. Gadea, A. Goasduff, D. Jelavić Malenica, N. Mărginean, G. Montagnoli, F. Scarlassara, N. Soić, A. M. Stefanini, C. A. Ur, and J. J. Valiente-Dobón, Eur. Phys. J. A **52**, 113 (2016).

[30] G. Montagnoli, F. Scarlassara, S. Beghini, A. Dal Bello, G. F. Segato, A. M. Stefanini, D. Ackermann, L. Corradi, J. H. He, and C. J. Lin, Nucl. Instrum. Methods Phys. Res. A **454**, 306 (2000).

[31] G. Pollarolo and A. Winther, Phys. Rev. C **62**, 054611 (2000).